JOURNAL OF QUATERNARY SCIENCE (2008)

Published online in Wiley InterScience
(www.interscience.wiley.com) DOI: 10.1002/jqs.1226

Preliminary ^{10}Be chronology for the last deglaciation of the western margin of the Greenland Ice Sheet

VINCENT RINTERKNECHT,[1]* YURI GOROKHOVICH,[2] JOERG SCHAEFER[1] and MARC CAFFEE[3]
[1] Lamont-Doherty Earth Observatory of Columbia University, Palisades, New York, USA
[2] Department of Environmental, Geographical and Geologic Sciences, Lehman College, City University of New York, Bronx, New York, USA
[3] Purdue Rare Isotope Measurement Laboratory and Department of Physics, Purdue University, West Lafayette, Indiana, USA

Rinterknecht, V., Gorokhovich, Y., Schaefer, J. and Caffee, M. Preliminary ^{10}Be chronology for the last deglaciation of the western margin of the Greenland Ice Sheet. *J. Quaternary Sci.*, (2008). ISSN 0267-8179.

Received 18 October 2007; Revised 30 May 2008; Accepted 9 June 2008

ABSTRACT: The now acknowledged thinning of the Greenland Ice Sheet raises concerns about its potential contribution to future sea level rise. In order to appreciate the full extent of its contribution to sea level rise, reconstruction of the ice sheet's most recent last deglaciation could provide key information on the timing and the height of the ice sheet at a time of rapid climate readjustment. We measured ^{10}Be concentrations in 12 samples collected along longitudinal and altitudinal transects from Sisimiut to within 10 km of the Isunguata Sermia Glacier ice margin on the western coast of Greenland. Along the longitudinal transect, we collected three perched boulders and two bedrocks. In addition, we sampled seven perched boulders along a vertical transect in a valley within 10 km of the Isunguata Sermia Glacier ice margin. Our pilot dataset constrains the height of the ice sheet during the Last Glacial Maximum (LGM) between 500 m and 840 m (including the 120 m relative sea level depression at the time of the LGM, 21 ka BP). From the transect we estimate the thinning of the ice sheet at the end of the deglaciation between 12.3 ± 1.5 ^{10}Be ka ($n = 2$) and 8.3 ± 1.2 ^{10}Be ka ($n = 3$) to be ~6 cm a^{-1} over this time period. Direct dating of the retreat of the western margin of the Greenland Ice Sheet has the potential to better constrain the retreat rate of the ice margin, the thickness of the former ice sheet as well as its response to climate change. Copyright © 2008 John Wiley & Sons, Ltd.

KEYWORDS: surface exposure dating; Greenland Ice Sheet; ice sheet height; last deglaciation.

Introduction

Palaeoclimatic trends in the polar region have become increasingly important following the recognition of a probable polar amplification to global warming (Huybrechts *et al.*, 2004). High-latitude feedback mechanisms play an important role in the climate system, but in the absence of long-term meteorological records natural climate variability and feedback mechanisms remain poorly understood. Arctic areas are rich in glacial features of all sizes and their deposition time and mode contain one of the few archives for deciphering past climate variability in present-day arid continental subarctic areas.

The dating of moraines and other glacial features through surface exposure dating (SED) is a major application of cosmogenic isotope analysis, with most studies focusing on the chronology of the associated glacier fluctuations and their broader climatic implications (Gosse *et al.*, 1995a; Stone *et al.*, 2003; Rinterknecht *et al.*, 2006, 2007). The largest ice-free land of western Greenland has a 175 km long eastward transect from the town of Sisimiut on the coast to the Isunguata Sermia Glacier ice margin. We used this transect to track the retreat of the Greenland Ice Sheet at the end of the last ice age. In addition, one of the glacial valleys was selected for large-scale dating and terrain mapping to investigate the important question of ice sheet thickness. Ice cover extended beyond (~100 km) the present-day coastline during the Hellefisk stage (Kelly, 1985). The deposition time of the Hellefisk moraine system is unknown but the massive morphology of the moraine stretching along the outer edge of the shelf (Brett and Zarudzki, 1979) suggests a possible deposition time during the Last Glacial Maximum (LGM) when sea level depression was at its maximum ca. 21 ka BP (Hanebuth *et al.*, 2000; Yokoyama *et al.*, 2000). During the course of deglaciation, the inland ice margin progressively receded over 175 km east in our study area (Fig. 1). The classic sequence of deglaciation suggests that halts or readvances interrupted the retreat and formed extensive moraine systems (Ten Brink, 1974; Van Tatenhove *et al.*, 1996):

* Correspondence to: V. Rinterknecht, School of Geography and Geosciences, University of St Andrews, Irvine Building, St Andrews, Fife KY16 9AL, UK.
E-mail: vr10@st-andrews.ac.uk

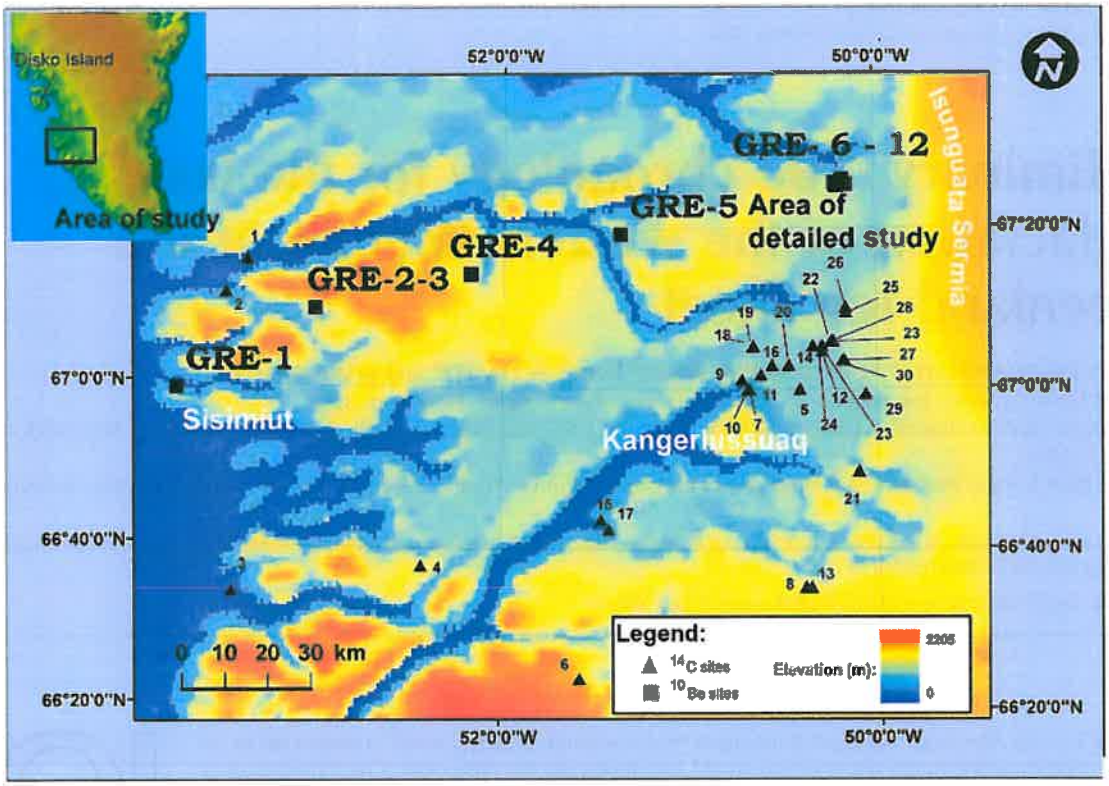

Figure 1 Study area with sampling sites (black squares) for surface exposure dating using ^{10}Be. The numbers associated with the radiocarbon sampling sites (black triangles) correspond to the location numbers in Table 1. The DEM is based on the GTOPO data (resolution of ~1 km, adapted from http://edc.usgs.gov/products/elevation/gtopo30/gtopo30.html, accessed 21 August 2007)

Sisimiut (located just offshore of the present coastline and assumed to be of Younger Dryas (YD) age), Taserqat, Sarfartôq/Advedtleq, Fjord, Umîvît/Keglen and Ørkendalen (close to the modern ice margin). These moraine systems were identified ~50 km south of Sisimiut, and dating and mapping studies are all but lacking in our study area.

We present here the first surface exposure ages for this sector of Greenland. These surface exposure ages constrain a preliminary chronology for the last deglaciation of the western margin of the Greenland Ice Sheet. These new data, together with existing radiocarbon ages and satellite imagery, complemented by our ground measurements and observations, define the chronological and geomorphological settings that allow us to reconstruct the pattern of the ice sheet margin recession as well as to constrain the thinning of the ice sheet through the last deglaciation.

Study area

The coastal region of Sisimiut together with the inland area in front of the Isunguata Sermia Glacier (Fig. 1) form the most extensive ice-free continuous land in southwestern Greenland (Weidick, 1995). This region is characterised by a gentle WSW–ENE trending hilly landscape reaching 300–700 m, with a few summits exceeding 1000 m above sea level (a.s.l.) where glacially abraded bedrock knolls alternate with extensive plains and large, bedrock-controlled lakes (Weidick, 1968; Willemse, 2002). Depositional features related to former ice expansion are widespread in the area and include moraines, thin patches of loose gravelly and sandy diamicton and scattered erratic boulders (Funder, 1989). Glaciofluvial and fluvial sediments, outwash plains and fluvial terraces cover the floors of all major valleys. Deglaciation and subsequent relative land uplift resulted in terraced proglacial sediments that grade downvalley from ice marginal deposits into emerged marine deltas in the valley mouths near the fjords (Ten Brink, 1974; Van Tatenhove *et al.*, 1996). The Holocene marine limit rises from approximately 40–60 m a.s.l. at the head of Kangerlussuaq to a position 130–140 m a.s.l. at the outer coast as a result of isostatic rebound (Willemse, 2002). Geodetic measurements in the region suggest that crustal subsidence is taking place due to a possible readvance of the ice margin 3–4 ka ago (Wahr *et al.*, 2001).

The lithology of the study area is dominated by Precambrian crystalline metamorphic rocks with a general ENE strike, belonging to the Nagssugtoqidian mobile belt (Willemse, 2002). The bedrock and derived erratic boulders consist mainly of granodioritic gneisses, a suitable lithology for ^{10}Be SED.

Ice cover extended beyond the present day coastline during the Sisimiut glaciation of Late Wisconsinan–Weichselian age (Funder, 1989). During the course of deglaciation, the inland ice margin progressively receded about 175 km in western Greenland. Frequent halts or readvances interrupted the retreat and formed extensive moraine systems (Ten Brink, 1972), including, from the marine shelf break to the present ice margin: the Hellefisk (tentatively associated with the LGM), the Sisimiut (tentatively associated with the YD), the Taserqat (first moraine system on the mainland), the Sarfartôq/Advedtleq, the Fjord, the Umîvît/Keglen, the Ørkendalen, an unnamed neoglacial moraine and the Little Ice Age moraine system. This moraine sequence provides one of the most complete geomorphological records for the Greenland deglaciation history (Van Tatenhove *et al.*, 1996; Forman *et al.*, 2007).

DOI: 10.1002/jqs

Fluctuation of the western Greenland Ice Sheet margin since the LGM

Based on morphological evidence (Brett and Zarudzki, 1979) and analogy with other areas around Greenland (Scoresby Sund and Kangerdlugssuaq in eastern Greenland), the LGM ice margin in western Greenland is materialised as a submerged moraine on the inner shelf (Kelly, 1985; Funder *et al.*, 2004). Further and firmer evidence on the last deglaciation history of the ice margin is found on land. The chronology of the emerged moraine sequence in western Greenland was first established by means of its relation to former relative sea level (Ten Brink, 1975). Emphasis was then placed on the collection of samples for radiocarbon dating to improve the determination of the moraine system ages (Table 1, Fig. 1). Based on radiocarbon dating of basal organic lake sediments the terrain was estimated to have been ice free as early as 9.2 ± 0.2 ^{14}C ka BP (10.4 ± 0.3 cal. ka BP; Kelly, 1979; site #1 in Fig. 1). An earlier deglacial estimate exists further north of the study area, north of Disko Island, where postglacial deposit (sample Ua-1789, 70.38° N, 54.95° W, 35 m a.s.l.) dates to 10.5 ± 0.1 ^{14}C ka BP (12.4 ± 0.2 cal. ka BP; Bennike *et al.*, 1994). These limiting radiocarbon ages suggest that the Sisimiut Moraine 40 km offshore could have been deposited during the YD. The oldest accelerator mass spectrometry (AMS) age obtained on organic deposits south-west of Kangerlussuaq (site #6 in Fig. 1) is 8.2 ± 0.1 ^{14}C ka BP (9.1 ± 0.1 cal. ka BP; Willemse, 2002), suggesting that deglaciation occurred rapidly by calving of the ice margin in the Søndre Strømfjord. Between ~6.0 and ~4.0 cal. ka BP the ice margin was behind its present position (Weidick *et al.*, 1990). The actual position of the ice margin is unknown, but circumstantial evidence exists for this recession: (1) a sharp contact exists between the present moraines and the proglacial tundra suggesting an ice sheet advance over a well-vegetated foreland; (2) aeolian deposits lying in front of the modern ice margin have an internal structure that imply a transport direction from east to west (Willemse *et al.*, 2003), with a source area of the material coming from sandur plains now covered by the Greenland Ice Sheet; (3) radiocarbon dated material from within these dunes is dated at 5.0 ± 0.1 ^{14}C ka BP (5.8 ± 0.1 cal. ka BP; Eisner *et al.*, 1995; site #20 in Fig. 1) suggesting large-scale redistribution of sandur sediments by wind well before 5.0 cal. ka BP; (4) measurement of the Greenland crust subsidence by means of global positioning system (GPS) is compatible with a retreat of the ice sheet margin followed by an advance of ~50 km (Wahr *et al.*, 2001; Dietrich *et al.*, 2005).

The recession was followed by a general readvance reported to begin at ca. 4.5–4.0 cal. ka BP (Anderson *et al.*, 1999). Optically stimulated luminescence (OSL) dates between ~3.0 and ~2.0 ka BP found on aeolian deposits on top of the neoglacial moraine south of the Isunguata Sermia glacier ice tongue suggest ice advance at this time (Forman *et al.*, 2007). Although the deglaciation history during the late Holocene (close to the modern ice margin) is fairly well constrained by AMS radiocarbon ages (Van Tatenhove *et al.*, 1996; sites #22, 23, 24, 27 in Fig. 1), and by OSL ages and lichenometry (Forman *et al.*, 2007), these ages give only minimum ages for the deglaciation history of this area. In addition, the time when

Table 1 Summary of relevant radiocarbon ages for the Holocene history of the research area

Lab ref.	Type of analysis	Material	Radiocarbon ages (^{14}C a BP)	Calibrated ages (cal. a BP)[a]	Latitude (° N)	Longitude (° W)	Site elevation (m a.s.l.)	Reference	Location no. in Fig. 1
I-10288	Conv.	Gyttja	9180 ± 200	10 420 ± 260	67.26	53.38	?	Kelly (1979)	1
K-1549	Conv.	Marine shells	9090 ± 140	10 230 ± 270	67.19	53.49	?	Kelly (1973)	2
K-1377	Conv.	Marine shells	9070 ± 160	10 250 ± 250	66.57	53.41	79	Weidick (1972)	3
UW-172	Conv.	Marine shells	8670 ± 100	9 710 ± 180	66.63	52.42	115	Ten Brink (1975)	4
K-1663	Conv.	Marine shells	8230 ± 140	9 220 ± 190	67.00	50.41	120	Weidick (1972)	5
UtC-5618	AMS	Organic deposit	8150 ± 60	9 120 ± 110	66.40	51.58	300	Willemse (2002)	6
UtC-3522	AMS	Marine shells	7500 ± 70	8 300 ± 90	67.00	50.68	21	Van Tatenhove *et al.* (1996)	7
AAR-3507	AMS	Gyttja	7210 ± 60	8 060 ± 100	66.59	50.39	155	Bennike (2000)	8
K-1664	Conv.	Marine shells	7140 ± 130	8 000 ± 160	67.02	50.72	58	Weidick (1972)	9
I-5512	Conv.	Marine shells	7025 ± 120	7 850 ± 120	67.00	50.69	10	Ten Brink (1975)	10
I-5589	Conv.	Marine shells	6505 ± 120	7 440 ± 130	67.03	50.62	31	Ten Brink (1975)	11
UtC-1987	AMS	Gyttja	6380 ± 100	7 300 ± 120	67.09	50.29	247	Van Tatenhove *et al.* (1996)	12
AAR-3514	AMS	Organic deposit	6120 ± 60	7 040 ± 130	66.59	50.36	150	Bennike (2000)	13
UtC-1990	AMS	Gyttja	6090 ± 50	7 020 ± 140	67.09	50.34	250	Van Tatenhove *et al.* (1996)	14
I-5506	Conv.	Marine shells	5850 ± 120	6 640 ± 140	66.73	51.47	10	Ten Brink (1975)	15
K-1715	Conv.	Marine shells	5630 ± 110	6 420 ± 120	67.05	50.56	15	Weidick (1972)	16
I-5510	Conv.	Marine shells	5620 ± 120	6 410 ± 120	66.71	51.43	4	Ten Brink (1975)	17
UtC-2535	AMS	Organic deposit	5280 ± 130	6 060 ± 140	67.09	50.66	200	Van Tatenhove *et al.* (1996)	18
UtC-2534	AMS	Wood fragment	5090 ± 70	5 830 ± 80	67.09	50.66	200	Van Tatenhove *et al.* (1996)	19
UtC-1586	AMS	Gyttja	5030 ± 60	5 780 ± 110	67.05	50.47	100	Eisner *et al.* (1995)	20
I-5587	Conv.	Marine shells	4340 ± 110	5 000 ± 270	66.83	50.10	2	Ten Brink (1975)	21
UtC-2034	AMS	Peat	4060 ± 60	4 620 ± 180	67.10	50.24	200	Van Tatenhove *et al.* (1996)	22
UtC-2035	AMS	Peat	3950 ± 60	4 410 ± 110	67.08	50.29	150	Van Tatenhove *et al.* (1996)	23
UtC-2033	AMS	Peat	3890 ± 50	4 330 ± 80	67.08	50.29	350	Van Tatenhove *et al.* (1996)	24
Ua-786	Conv.	Organic deposit	3230 ± 110	3 480 ± 140	67.16	50.16	?	Östmark (1988)	25
Ua-616	Conv.	Organic deposit	2660 ± 90	2 770 ± 150	67.17	50.16	?	Östmark (1988)	26
UtC-2537	AMS	Gyttja	2010 ± 80	1 990 ± 110	67.06	50.17	250	Van Tatenhove *et al.* (1996)	27
St-10179	Conv.	Organic deposit	630 ± 110	610 ± 110	67.10	50.23	?	Ericson (1987)	28
UW-180	Conv.	Organic deposit	330 ± 80	390 ± 80	66.99	50.06	?	Ten Brink (1975)	29
UtC-2536	AMS	Wood fragment	0 ± 50	—	67.06	50.18	250	Van Tatenhove *et al.* (1996)	30

[a] Calibration was performed using IntCal04 (Reimer *et al.*, 2004). Errors correspond to one standard deviation.

DOI: 10.1002/jqs

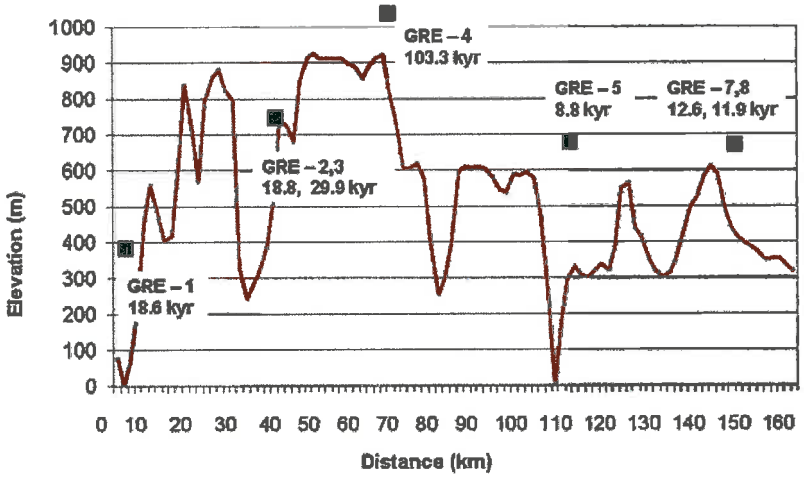

Figure 2 Altitudinal profile along a transect from Sisimiut to the ice margin and passing through the sampling sites (black squares). Our sampling sites are virtually 'floating' above the topographic profile. This effect illustrates the difference existing between the poorly resolved topographic data (GTOPO is the best available data in our study area) used to build DEM and the high-resolution data we measured for our sampling sites using a GPS (sub-metre Trimble XT)

the coastal region was first deglaciated remains elusive as most of the shells were dated by conventional techniques (requiring multiple shells for one analysis), thus limiting the reliability of the results (Bennike and Björck, 2002). Similar difficulties to identify the ice retreat dynamics have been reported further north in the Jakobshavn Isbræ fjord (Long *et al.*, 2006).

^{10}Be chronology

Methods

We sampled 12 surfaces (Figs 1 and 2): five along a longitudinal transect that is parallel to the general retreat direction of the western margin of the Greenland Ice Sheet, and seven in the valley near the ice margin (Fig. 3). Beryllium (Be) was extracted from quartz following a modified version of the procedures given in Kohl and Nishiizumi (1992) and Rinterknecht (2003). The non-magnetic sample fraction (grain size between 0.25 and 0.71 mm) was first boiled in pyrophosphoric acid to dissolve most of the aluminosilicates. The grain size fraction was then leached repeatedly with solutions of HNO_3 and HF until satisfactory quartz purity was reached. A reference 0.20 mg ^{9}Be spike was added to each sample. We used anion exchange, cation exchange, and selective precipitation techniques to progressively isolate the Be. ^{10}Be/^{9}Be ratios were measured by AMS at the PRIME Laboratory facility, Purdue University (Jackson *et al.*, 2004), relative to the Nishiizumi standards Be 0152 (for sample GRE-1) and Be 0153 (for all other samples). Converting ^{10}Be concentrations to exposure ages requires the

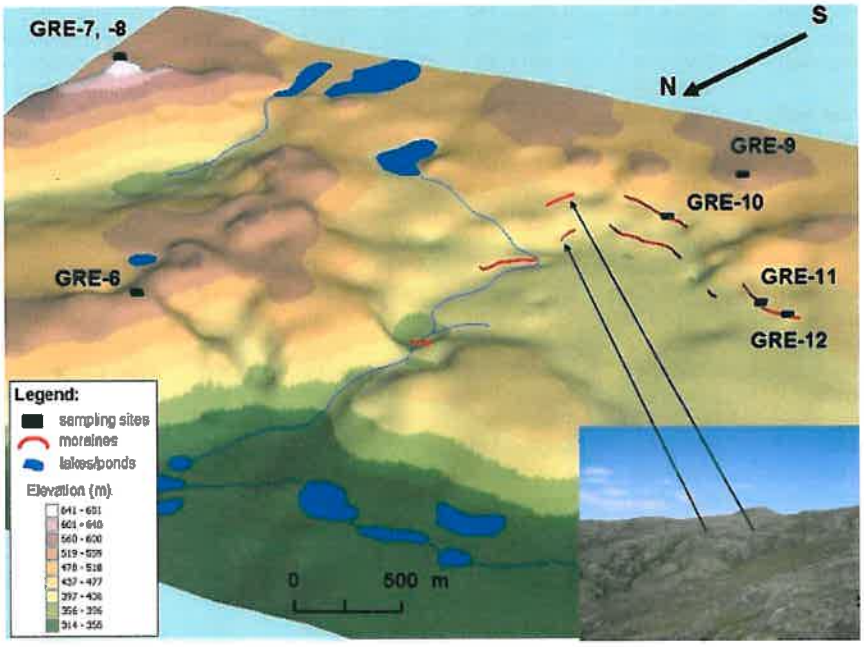

Figure 3 Reconstructed DEM (see text for details) of the study area close to the ice margin with sampling sites for SED (black squares). Red lines indicate the moraine segments found in the valley and surveyed on the ground by means of GPS

DOI: 10.1002/jqs

use of an effective ^{10}Be production rate. We adopt here a value of 5.1 atoms g^{-1} a^{-1} (Stone, 2000). This production rate, effective for sea level (1013.25 hPa) and high latitudes (>60°), was scaled to the 'effective' elevation and geographic latitude of each sample using Stone's factors (Stone, 2000). Since there is still no consensus regarding these parameters, or their uncertainties, we choose here to report our ages as ^{10}Be ages (Gosse *et al.*, 1995a). All our samples are located at ~67° N, which implies a correction for the palaeomagnetic effect of less than 1% for the production rate (Masarik *et al.*, 2001). We chose not to apply the correction for this potential variability of the palaeomagnetic field intensity.

We thus consider only sample- or site-specific uncertainties: topographic shielding, snow cover, sample thickness, and erosion. Shielding by surrounding relief is excluded since the samples come from the highest elevation in the region. Because of their dominant position in the landscape we assume that any snow would have blown off rapidly after storms and thus we do not correct for snow cover. Alternatively, if we assume snow cover of 50 cm for four months per year, the production would be reduced by only ~2%. We used the model of Lal (1991) to correct the production rate for sample thickness. We corrected the production rate for as much as 2%. Most of the samples display either rough surfaces with emergent resistant quartz grains or surfaces that retain glacial polish, indicating little to no erosion. The surface of sample GRE-2 appears more highly weathered and could have experienced greater erosion (i.e. slab erosion); this is supported by our sample analysis, as the age is significantly younger than the age of sample GRE-3 obtained on a glacially polished quartz vein protruding from the bedrock (Table 2). To estimate the possible effect of erosion on surface exposure ages, we assumed an erosion rate of 1.3 mm ka^{-1} estimated by Gosse *et al.* (1995b) for granite in the western USA. Introducing this erosion rate would increase the exposure ages by 1.2–1.5%. We report the exposure ages without including the erosion parameter.

Because of the elevation dependence of the ^{10}Be production rate, we should account for the elevation variation through time as a consequence of glacioisostatic uplift. Western Greenland is still undergoing post-deglacial isostatic rebound, with modern lithosphere responses ranging from −3.1 mm a^{-1} (which corresponds to subsidence) in Kangerlussuaq to 1 mm a^{-1} in Sisimiut (Dietrich *et al.*, 2005). During the Holocene, local sea level records of isostatic uplift suggest that marine limits rose from 40–60 m a.s.l. in Kangerlussuaq to 130–140 m a.s.l. near Sisimiut (Willemse, 2002). Based on these estimates we infer that samples near the modern coastline have experienced the largest elevation variation through time compared to samples near the modern ice margin. Accordingly, the production rate used to calculate surface exposure ages near the coast should experience the largest correction compared to the production rate used to calculate exposure ages near the ice margin. Although a subsidence rate is measured in Kangerlussuaq (Dietrich *et al.*, 2005), it is not possible to account for the total subsidence that has taken place since the ice margin readvanced ca. 4 ka ago. As a result, we chose not to take into account the glacioisostatic uplift effect and we present here minimum exposure ages.

Results

Our ^{10}Be ages range from 7.2 ± 1.3 to 103.3 ± 3.8 ^{10}Be ka (Table 2). We interpret our exposure ages as the time when the ice retreated from the landscape and thus the time when the underlying bedrock and erratic boulders were first subject to cosmogenic nuclide accumulation. Based on the sample positions with respect to their longitude and elevation, the exposure ages suggest a simple final retreat history for the ice margin from the modern coastline to about 10 km from the modern ice margin (Fig. 1). Two perched boulders on bedrock, GRE-5 (8.8 ± 3.5 ^{10}Be ka) and GRE-6 (7.2 ± 1.3 ^{10}Be ka), are anomalously young and do not fit the general retreat pattern. Although we are aware that some polar landscapes could have been preserved under cold-based ice (Briner *et al.*, 2005, 2007),

Table 2 Sample characteristics and ^{10}Be exposure ages from the western sector of the Greenland Ice Sheet

Sample ID	Height above ground (m)[a]	Quartz (g)	Latitude (° N)	Longitude (° W)	Elevation (m a.s.l.)	[^{10}Be] (10^4 atoms g^{-1})[b]	Scaling factor[c]	Thickness factor	Corrected production rate (atoms a^{-1} g^{-1})[d]	Exposure age (^{10}Be ka)[e]
GRE-1	1.0	19.994	66.988	53.736	385	13.5 ± 3.6	1.48	0.97	7.3	18.6 ± 4.9
GRE-2	2.0	15.076	67.162	53.008	721	18.4 ± 3.4	2.00	0.96	9.8	18.8 ± 3.5
GRE-3	0.0	15.019	67.162	53.008	721	29.1 ± 1.3	2.00	0.96	9.8	29.9 ± 1.4
GRE-4	0.0	15.206	67.238	52.174	1118	140.8 ± 5.3	2.80	0.98	14.0	103.3 ± 3.8
GRE-5	0.8	20.004	67.323	51.369	687	8.3 ± 3.3	1.94	0.95	9.5	8.8 ± 3.5
GRE-6	2.1	30.094	67.437	50.171	576	6.3 ± 1.1	1.76	0.97	8.7	7.2 ± 1.3
GRE-7	0.4	30.033	67.426	50.152	682	11.9 ± 1.5	1.93	0.96	9.5	12.6 ± 1.5
GRE-8	0.8	30.130	67.426	50.152	682	11.4 ± 1.4	1.93	0.97	9.6	11.9 ± 1.4
GRE-9	1.4	35.048	67.424	50.205	539	7.9 ± 0.5	1.70	0.97	8.4	9.4 ± 0.6
GRE-10	3.1	40.072	67.425	50.201	442	6.0 ± 1.3	1.56	0.98	7.8	7.7 ± 1.7
GRE-11	1.9	40.012	67.429	50.211	439	6.4 ± 0.9	1.55	0.96	7.6	8.4 ± 1.2
GRE-12	1.8	40.005	67.429	50.213	437	6.7 ± 0.5	1.55	0.98	7.7	8.7 ± 0.6

[a] Height of zero metres corresponds to bedrock sample.
[b] ^{10}Be/^{9}Be ratios were measured at the PRIME Lab facility, relative to the Nishiizumi standards Be 0152 (for sample GRE-1) and Be 0153 (for all other samples).
[c] Scaling factor accounts for the mode of production of ^{10}Be atoms at the boulder surface: 97.8% by spallation.
[d] We used an assumed production rate of 5.1 atoms g^{-1} a^{-1} scaled for each sample location following Stone's (2000) method, and corrected for sample thickness following Lal's (1991) method.
[e] Analytical uncertainties (propagated at ± 1σ level) include a procedural blank of 1.32 ± 0.12 × 10^4 atoms g^{-1} for samples GRE-2 to GRE-12 and of 0.76 ± 0.54 10^4 atoms g^{-1} for sample GRE-1. Most of the exposure ages have an analytical error larger (range 4–40%, mean of 15%) than what is routinely expected from AMS facilities (3–4%). Most samples had very low ^{9}Be currents, resulting in few ^{10}Be events, and high analytical uncertainties. A possible explanation could be found in the rather large quartz samples processed with significant Al background.

DOI: 10.1002/jqs

the anomalously young exposure ages for samples GRE-5 and GRE-6 cannot be explained by this effect. Because these two perched boulders display fresh surfaces with no obvious erosion signs, we suggest that these boulders may have been subject to post-depositional movements or that melting of dead ice could have delayed their exposure.

Combining our new ^{10}Be data with existing radiocarbon ages on postglacial organic matter (Table 1), we constrain the chronology of the ice margin retreat and the height of the ice sheet for the central western sector of the Greenland Ice Sheet during the last deglaciation.

Three radiocarbon ages (sites 1–3, Table 1, Fig. 1) point to a minimum deglaciation time of the area between 9.2 ± 0.2 and 9.1 ± 0.2 ^{14}C ka BP (10.4 ± 0.3 and 10.2 ± 0.3 cal ka BP, respectively). In addition, considering the AMS radiocarbon age obtained on marine shells north of Disko Island, the present coastline may have been ice free as early as 10.5 ± 0.1 ^{14}C ka BP (12.4 ± 0.2 cal ka BP; Bennike *et al.*, 1994). Samples GRE-1 to GRE-5 were taken at single stops during a helicopter flight and provide a chronological discrete reference that can be used as a proxy for deglaciation timing. Sample GRE-1 (18.6 ± 5.0 ka; the error includes a 6% uncertainty in the production rate; Stone, 2000) suggests a deglaciation time for the Sisimiut coastal region much earlier than what the radiocarbon age constrains: 12.4 ± 0.2 cal. ka BP. The difference could be explained by a low-profile ice sheet margin at the time of the Sisimiut stage where ice tongues would have been confined to fjords, leaving higher inter-fjords regions such as the site where GRE-1 was sampled (i.e. 385 m) ice free.

The deposition time of sample GRE-2 (18.8 ± 3.5 ^{10}Be ka), located 2 m apart from sample GRE-3 (29.9 ± 1.4 ^{10}Be ka), likely represents a minimum age as the boulder displays signs of heavy weathering (debris accumulation is present at the base of the boulder). Sample GRE-3 comes from a glacially polished quartz vein protruding from the bedrock and we thus take this exposure age as the best estimate compare to GRE-2 for the time of ice retreat. In order to make sample GRE-2 as old as GRE-3, the erosion rate on sample GRE-2 should have been ~22 mm ka^{-1}. This high erosion rate estimate is plausible given that sample GRE-2 comes from a grusified boulder showing signs of ventifaction on its flanks.

Sample GRE-4 (103.3 ± 3.8 ^{10}Be ka) suggests that the plateau was ice free since at least the end of Marine Isotope Stage 6, when the ice volume on land reached its maximum prior to the LGM (Waelbroeck *et al.*, 2002). Based on our available data and on the glacial erosion marks left by the ice sheet – glacial polish in the case of sample GRE-3 and glacial grooves (e.g. p-forms carved by abrasion and melt water) in the case of sample GRE-4 – we interpret the exposure ages to reflect the last time the ice sheet retreated from these sites.

Sample GRE-5 (8.8 ± 3.5 ^{10}Be ka) rests on a plateau-like hill (at 687 m), and the comparatively older exposure ages of samples GRE-7 and GRE-8 (12.6 ± 1.5 ^{10}Be ka and 11.9 ± 1.4 ^{10}Be ka respectively) located at a similar elevation but 40 km inland point to a possible melting of dead ice at the sample GRE-5 site. Alternatively, the young exposure age could be explained by post-depositional movement of the boulder.

Samples GRE-6 to GRE-12 were taken during a three-day ground survey, which allowed us to take an altitudinal transect in our study area (Fig. 3). Elevations in the study area were measured along several vertical profiles using the GPS Trimble GeoXT. These data, combined with Landsat image and verified by photos taken in the field, allowed rendering of the 3D digital elevation model (DEM) depicted in Fig. 3. Sample GRE-6 rests on a plateau-like hill (at 576 m), and the comparatively young exposure age within our altitudinal transect (Fig. 4) could reflect post-depositional movement. Alternatively, the young exposure age could be explained by melting of dead ice after the main retreat of the ice margin.

We sampled two perched boulders on the highest point (682 m) of an unnamed valley in the study area. The mean exposure age of samples GRE-7 (12.6 ± 1.5 ^{10}Be ka) and GRE-8 (11.9 ± 1.4 ^{10}Be ka) is 12.3 ± 0.3 ^{10}Be ka (the error corresponds to the standard deviation of the mean exposure age). Sample GRE-9 (9.4 ± 0.6 ^{10}Be ka) was taken at an elevation of 539 m. Samples GRE-10 (7.7 ± 1.7 ^{10}Be ka), GRE-11 (8.4 ± 1.2 ^{10}Be ka) and GRE-12 (8.7 ± 0.6 ^{10}Be ka) come from the same moraine (at ~440 m) and we calculated a mean deposition time of 8.3 ± 0.3 ^{10}Be ka (the error corresponds to the standard deviation of the mean exposure age). Together (excluding sample GRE-6), these samples show decreasing exposure ages with decreasing altitude (Fig. 4), i.e. the chronology is in stratigraphic order and reflects the successive thinning of the covering ice sheet. Our altitudinal transect from 682 m to 440 m suggests a thinning of the ice sheet of ~240 m in 4 ka, or a thinning rate of ~6 cm a^{-1}.

Based on our new exposure ages and on existing radiocarbon ages we calculated ice retreat rates between 12.4 cal. ka BP and 8.3 ^{10}Be ka and between 8.3 ^{10}Be ka and ca. 4.5 cal. ka BP. We first consider the Sisimiut Moraine to be a moraine deposited during the Lateglacial and assigned it an age of 12.4 cal. ka BP. The first firm overlap between our exposure ages and the radiocarbon ages occurs ~20 km to the present ice margin position. Our mean exposure age of 8.3 ± 0.6 ka (n = 3, the error includes a 6% uncertainty in the production rate; Stone, 2000) is in good agreement with the age of the Umîvît/Keglen moraine system formation 8.3 ± 0.1 cal. ka BP to 7.4 ± 0.1 cal. ka BP (sites 7–10, Table 1, Fig. 1) assigned by Van Tatenhove *et al.* (1996). We calculated a retreat rate of 48 m a^{-1} over this section of the ice-free area. From 8.3 ka the ice margin retreated progressively during the Holocene, as supported by the radiocarbon ages (sites 11–30, Table 1, Fig. 1), and mounting evidence is pointing to an ice margin retreat further inland than the present position before readvancing. The exact position of the palaeo-ice margin is unknown but continuous GPS measurements record subsidence in a region that should display uplift motion if the ice sheet had been retreating steadily since the early Holocene. To reconcile the observed subsidence with the ice margin history, ice dynamical models support a readvance of the ice margin of ~50 km in the last 4.5 ka (Wahr *et al.*, 2001). We calculated a retreat rate of 18 m a^{-1} for the ice margin between 8.3 ^{10}Be ka and 4.5 cal. ka BP. The vast change in retreat rates before and after 8.3 ^{10}Be ka could be best explained by differences in ice retreat mechanisms. Rapid deglaciation can be achieved by calving in fjords (Funder and Hansen, 1996; Bennike and Björck, 2002). Further inland, where the fjords are becoming increasingly narrower, the deglaciation would have been achieved at a slower pace by ablation of land-based ice.

Discussion and conclusion

Deglaciation sequence

Exposure ages become progressively younger from the coastline towards the modern ice margin, again suggesting a strong consistency between the chronology and the stratigraphy. However, our preliminary chronology based on SED does not allow us to conclude on a simple retreat of the ice sheet during the last deglaciation, as suggested by the classic representation

DOI: 10.1002/jqs

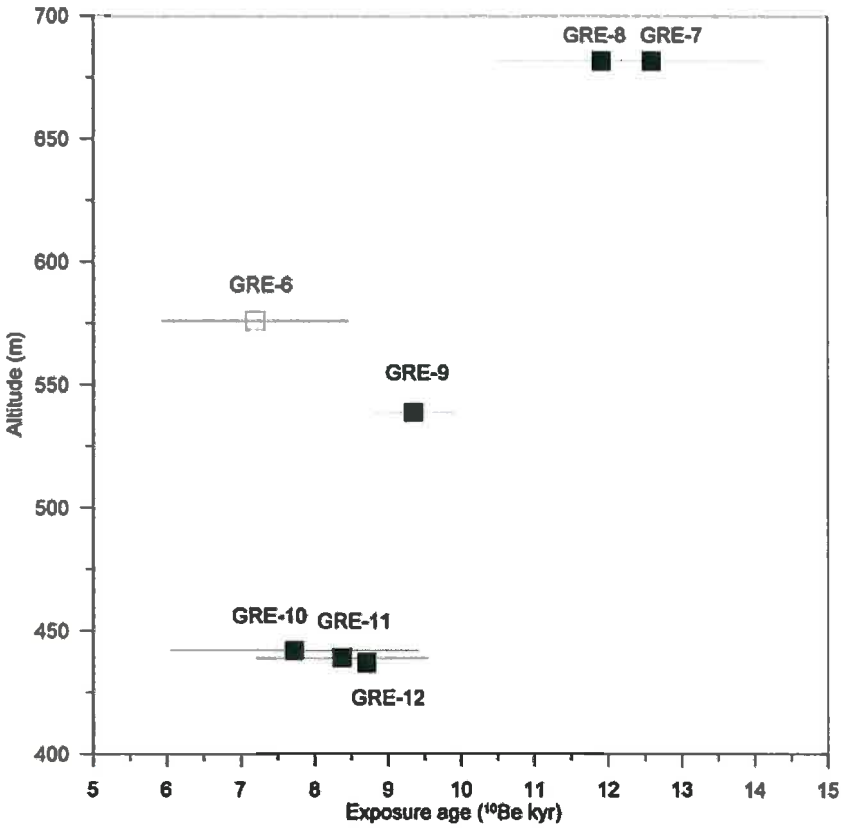

Figure 4 Exposure ages (analytical uncertainties propagated at 1σ level) of glacially transported erratic boulders plotted *versus* their respective altitude. Black squares are data included in the calculation of the ice sheet thinning. The open square is a sample coming from a plateau-like area detached from the main drainage system from which the other samples were taken (Fig. 3). The exposure age could reflect a different deglaciation history from the one from the adjacent valley. The exposure age could reflect a different deglaciation history than the one from the adjacent valley

of the moraine sequence in the region. We note that from our helicopter flight between the coastline and our detailed study area close to the ice margin the classic moraine sequence as described by Ten Brink (1975) and Van Tatenhove *et al.* (1996) was less than obvious. In fact no moraines at all were to be identified in this area. We provide two possible explanations for this disagreement. First, details like lateral and end moraines may have eluded us while flying above the landscape and these features would require a ground survey to be able to identify them. Second, the moraine sequence as originally defined by Ten Brink (1974, 1975) may not be based on distinct moraines in the landscape but rather reflect a hypothetical classification based on (1) a continuous glacial drift deposited during the ice sheet retreat and (2) the relation of this glacial drift to radiocarbon ages determined on marine limits (Van Tatenhove *et al.*, 1996). Van Tatenhove *et al.* (1995) clearly pointed out that the correlation between the radiocarbon ages (obtained from uplifted shorelines in fjords (Fig. 1)) used to constrain the moraine sequence chronology and the moraine system itself is unclear. We thus suggest that the last deglaciation history of western Greenland might greatly benefit from additional larger-scale exposure dating campaigns: first we would be able to date moraine deposition directly; and second, SED would eliminate speculation on the relationship between radiocarbon-dated marine limits and time of moraine formation. The result would be a robust direct chronology (using ^{10}Be) for the deglaciation of the western margin of the Greenland Ice Sheet. In addition, mapping of the study area would greatly benefit from a finer-scale mapping campaign to improve the resolution of the mapping necessary to interpret the glacial/deglacial history of the region. To date, the best available topography is derived from GTOPO (resolution of ~1 km) and the agreement between these data and our field measurements is poor (Fig. 2).

In our detailed study area we found two parallel moraines nested on the flank of an unnamed valley that we visited during our ground survey (Fig. 3). According to our exposure ages this moraine was deposited at 8.3 ± 0.3 ^{10}Be ka ($n = 3$).

The rates at which the ice sheet margin retreated before ($48\,m\,a^{-1}$) and after ($18\,m\,a^{-1}$) 8.3 ± 0.3 ^{10}Be ka suggest that the ice sheet retreat was mostly influenced by the local topography. Near the modern coastline, thin ice streams (as constrained by sample GRE-1 exposure age and radiocarbon ages), directly in contact with shallow continental shelf waters, were prone to rapid retreat via a calving mechanism. Further inland, as the fjords are progressively replaced by plateau-like landscape, the ice sheet rests increasingly on the bedrock. In such a topographic setting the principal mechanism for ice margin retreat would have occurred by ablation.

In addition, based on the clustering of exposure ages at 8.3 ± 0.3 ^{10}Be ka on the only set of moraines found so far, we speculate that the ice margin in this sector of western Greenland could have potentially stagnated in response to the 8.2 ka cold event (Alley and Ágústsdóttir, 2005; Long *et al.*, 2006; Thomas *et al.*, 2007) during its overall general retreat.

Height of the ice sheet

Ice sheet geometry is crucial to calculate the potential contribution to past, present and future sea level variations

DOI: 10.1002/jqs

due to water release or sequestration by ice sheets. The former extent of an ice sheet is usually available through the presence of moraines, but a missing crucial parameter in past ice sheet reconstruction is often the height of the ice sheet itself. SED has the potential to offer information on past ice sheet geometry, both on its former extent and on its height at a specific time (Brook *et al.*, 1996; Stone *et al.*, 2003; Goehring *et al.*, 2008).

In western Greenland the maximum extent of the ice sheet on the shelf is known through sparker and boomer surveys off the coast (Brett and Zarudzki, 1979). Although the time of deposition of this moraine system is unknown, based on the available onshore deglacial chronology, the LGM could potentially represent a good estimate (Kelly, 1985). Based on our surface exposure ages, samples GRE-3 and GRE-1 provide information on the maximum height of the ice sheet. The location of sample GRE-3 (29.9 ± 1.4 ^{10}Be ka) suggests a maximum height the ice sheet could have reached during the LGM. Sample GRE-3 comes from the bedrock that could have been subject to a complex exposure and burial history. However, based on the result of sample GRE-2 (18.8 ± 3.5 ^{10}Be ka), a highly weathered boulder, which provides a very minimum age for the deglaciation of the area, we exclude the possibility that the ice sheet covered this area during the LGM. Because sample GRE-3 was not covered by ice during the LGM, the ice sheet reached a maximum altitude of ~720 m. Sample GRE-1 (18.6 ± 4.9 ^{10}Be ka) was exposed towards the end of the LGM and its location suggests that the modern coastline was ice free above 385 m. Both samples, GRE-3 and GRE-1, provide a minimum and a maximum constraint on the ice sheet height during the LGM: between 385 m and 720 m.

If we consider the global relative sea level (RSL) to have been depressed by ~120 m during the LGM (Yokoyama *et al.*, 2000; Hanebuth *et al.*, 2000), the ice thickness would have been not greater than ~505 m and not less than ~840 m. Similarly, the ice thickness would have been less than ~505 m at the end of the LGM. Furthermore, if we assume that the position of the maximum extent of the LGM is effectively at the outer edge of the shelf, the ice thickness estimates suggest that a thin ice sheet stretched up to the continental shelf ~100 km from the modern coastline, consistent with an ice sheet drainage system controlled by ice streams.

In the case of the Sisimiut Moraine located 40 km offshore, taking the oldest AMS radiocarbon age and our exposure age for sample GRE-1 at face value would support a low-profile ice sheet, possibly confined to the fjords at the time of the Sisimiut Moraine formation. The moraine is tentatively correlated to the YD cold event, which corresponds roughly to the exposure ages we obtained on two boulders (samples GRE-7 and GRE-8) located inland 190 km from the Sisimiut Moraine at an elevation of 680 m. The low ice sheet profile sloping at ~3.6 m km^{-1} along our transect would have reached an elevation of 140 m near the cost, leaving the GRE-1 sampling site (385 m) as a nunatak since the end of the LGM.

Further inland, our altitudinal transect (Fig. 4) provides information on the thinning of the ice sheet between 12.3 ± 0.3 ^{10}Be ka ($n = 2$) and 8.3 ± 0.3 ^{10}Be ka ($n = 3$). Stone *et al.* (2003) demonstrated the validity of such an interpretation for the deglaciation history of the West Antarctica Ice Sheet. We calculated a thinning rate range of ~4–8 cm a^{-1} for this sector of the western coast of Greenland. This thinning rate calculated between the end of the last deglaciation and the beginning of the Holocene corresponds to the lower end of the modern thinning rate range measured for this sector of the ice sheet margin (10–40 cm a^{-1}; Krabill *et al.*, 2004).

Our constraints on the ice sheet thickness and the rate of ice margin retreat suggest that the western Greenland Ice Sheet was thin enough to respond rapidly to improving climatic conditions at the end of the LGM and during the Lateglacial–early Holocene. The rapid deglaciation is supported to some extent by radiocarbon ages in fjord areas (Willemse, 2002). A series of altitudinal profiles dated by means of SED would improve our understanding of some of the key questions of the Greenland Ice Sheet dynamics during the last deglaciation.

Acknowledgements The NSF Office of Polar Programs sponsored the travel to and from Kangerlussuaq. Logistic support in Greenland was provided by Veco Polar Resources; special thanks to Robin Abbot. Support for fieldwork and helicopter time was provided by the Comer Science and Education Foundation and the Climate Center of the Lamont-Doherty Earth Observatory of Columbia University. Thanks to Ms Patricia Ahmetaj, who kindly provided the Trimble GPS GeoXT for field mapping. Henrik (our helicopter pilot) provided the necessary flexibility and help during our work along the transect. AMS analyses were conducted by PRIME Lab under the free seed analysis program. This is LDEO contribution #7177.

References

Alley RB, Ágústsdóttir AM. 2005. The 8K event: cause and consequences of a major Holocene abrupt climate change. *Quaternary Science Reviews* **24**: 1123–1149.

Anderson NJ, Bennike O, Christoffersen K, Jeppesen E, Markager S, Miller G, Renberg I. 1999. Limnological and palaeolimnological studies of lakes in southwestern Greenland. *Geology of Greenland Survey Bulletin* **183**: 68–74.

Bennike O. 2000. Palaeoecological studies of Holocene lake sediments from west Greenland. *Palaeogeography, Palaeoclimatology, Palaeoecology* **155**: 285–304.

Bennike O, Björck S. 2002. Chronology of the last recession of the Greenland Ice Sheet. *Journal of Quaternary Science* **17**: 211–219.

Bennike O, Hansen KB, Knudsen KL, Penny DN, Rasmussen KL. 1994. Quaternary marine stratigraphy and geochronology in central west Greenland. *Boreas* **23**: 194–215.

Brett CP, Zarudzki EFK. 1979. *Project Westmar, a shallow marine geophysical survey on West Greenland continental shelf.* Rapport 87, Grønlands Geologiske Undersøgelse, Copenhagen; 27 pp.

Briner JP, Miller GH, Davis PT, Finkel R. 2005. Cosmogenic exposure dating in arctic glacial landscapes: implications for the glacial history of northeastern Baffin Island, Arctic Canada. *Canadian Journal of Earth Sciences* **42**: 67–84.

Briner JP, Overeem I, Miller GH, Finkel R. 2007. The deglaciation of Clyde Inlet, northeastern Baffin Island, Arctic Canada. *Journal of Quaternary Science* **22**: 223–232.

Brook EJ, Nesje A, Lehman SJ, Raisbeck GM, Yiou F. 1996. Cosmogenic nuclide exposure ages along a vertical transect in western Norway: implications for the height of the Fennoscandian ice sheet. *Geology* **24**: 207–210.

Dietrich R, Rülke A, Scheinert M. 2005. Present-day vertical crustal deformations in West Greenland from repeated GPS observations. *Geophysical Journal International* **163**: 865–874.

Eisner WR, Törnqvist TE, Koster EA, Bennike O, Van Leeuwen JFN. 1995. Paleoecological studies of a Holocene lacustrine record from the Kangerlussuaq (Søndre Strømfjord) region of West Greenland. *Quaternary International* **43**: 55–66.

Ericson KI. 1987. *Environments and processes of deposition of till-like sediments at the margin of Russels Glacier near Sondre Stromfjord, West Greenland.* Report 9, University of Stockholm, Department of Quaternary Research, Stockholm.

Forman SL, Marin L, Van Der Veen C, Tremper C, Csatho B. 2007. Little Ice Age and neoglacial landforms at the Inland Ice margin, Isunguata Sermia, Kangerlussuaq, west Greenland. *Boreas* **36**: 341–351.

Funder S. 1989. Quaternary geology of the ice-free areas and adjacent shelves of Greenland. In *Geology of Canada*, No. 1: *Quaternary Geology of Canada and Greenland*, Fulton RJ (ed.). Geological Survey of Canada: Ottawa; 743–792.

Funder S, Hansen L. 1996. The Greenland ice sheet: a model for its culmination and decay during and after the last glacial maximum. *Bulletin of the Geological Society of Denmark* **42**: 137–152.

Funder S, Jennings A, Kelly M. 2004. Middle and late Quaternary glacial limits in Greenland. In *Quaternary Glaciations: Extent and Chronology*, Part II, Ehlers J, Gibbard PL (eds). Elsevier: Amsterdam; 425–430.

Goehring BM, Brook EJ, Linge H, Raisbeck GM, Yiou F. 2008. Beryllium-10 exposure ages of erratic boulders in southern Norway and implications for the history of the Fennoscandian Ice Sheet. *Quaternary Science Reviews* **27**: 320–336.

Gosse JC, Klein J, Evenson EB, Lawn B, Middleton R. 1995a. Beryllium-10 dating of the duration and retreat of the Last Pinedale glacial sequence. *Science* **268**: 1329–1333.

Gosse JC, Evenson EB, Klein J, Lawn B, Middleton R. 1995b. Precise cosmogenic ^{10}Be measurements in western North America: support for a global Younger Dryas cooling event. *Geology* **23**: 877–880.

Hanebuth T, Stattegger K, Grootes PM. 2000. Rapid flooding of the Sunda Shelf: a Late-Glacial sea-level record. *Science* **288**: 1033–1035.

Huybrechts P, Gregory J, Janssens I, Wild M. 2004. Modelling Antarctic and Greenland volume changes during the 20th and 21st centuries forced by GCM time slice integrations. *Global and Planetary Change* **42**: 83–105.

Jackson GS, Elmore D, Caffee M, Mueller KA, De Bonte B, Muzikar P, Alexander B. 2004. Ion source modeling and design at PRIME Lab. *Nuclear Instruments and Methods in Physics Research B* **223–224**: 155–160.

Kelly M. 1973. *Radiocarbon dated shell samples from Nordre Strømfjord, West Greenland.* Rapport 59, Grønlands Geologiske Undersøgelse, Copenhagen.

Kelly M. 1979. *Comments on the implications of new radiocarbon dates from the Holsteinsborg region, central West Greenland.* Rapport 95, Grønlands Geologiske Undersøgelse, Copenhagen; 35–42.

Kelly M. 1985. A review of the Quaternary geology of western Greenland. In *Quaternary Environments in Eastern Canadian Arctic, Baffin Bay, and Western Greenland*, Andrews JT (ed.). Allen & Unwin: Boston, MA; 461–501.

Kohl CP, Nishiizumi K. 1992. Chemical isolation of quartz for measurement of *in-situ*-produced cosmogenic nuclides. *Geochimica et Cosmochimica Acta* **56**: 3583–3587.

Krabill W, Hanna E, Huybrechts P, Abdalati W, Cappelen J, Csatho B, Frederick E, Manizade S, Martin C, Sonntag J, Swift R, Thomas R, Yungel J. 2004. Greenland Ice Sheet: increased coastal thinning. *Geophysical Research Letters* **31**: 1–4.

Lal D. 1991. Cosmic ray labeling of erosion surfaces: *in situ* nuclide production rates and erosion models. *Earth and Planetary Science Letters* **104**: 424–439.

Long AJ, Roberts DH, Dawson AG. 2006. Early Holocene history of the west Greenland Ice Sheet and the GH-8.2 event. *Quaternary Science Reviews* **25**: 904–922.

Masarik J, Frank M, Schäfer JM, Wieler R. 2001. Correction of in situ nuclide production rates for geomagnetic field intensity variations during the past 800,000 years. *Geochimica et Cosmochimica Acta* **65**: 2995–3003.

Östmark KIE. 1988. *Till genesis in areas of crystalline bedrock with undulating topography: examples from west Greenland and central Sweden.* Report 11, Department of Quaternary Research, University of Stockholm, Stockholm.

Reimer PJ, Baillie MGL, Bard E, Bayliss A, Beck JW, Bertrand CJH, Blackwell PG, Buck CE, Burr GS, Cutler KB, Damon PE, Edwards RL, Fairbanks RG, Friedrich M, Guilderson TP, Hogg AG, Hughen KA, Kromer B, McCormac FG, Manning SW, Ramsey CB, Reimer RW, Remmele S, Southon JR, Stuiver M, Talamo S, Taylor FW, van der Plicht J, Weyhenmeyer CE. 2004. IntCal04 Terrestrial radiocarbon age calibration, 26–0 ka BP. *Radiocarbon* **46**: 1029–1058.

Rinterknecht VR. 2003. *Cosmogenic ^{10}Be chronology for the last deglaciation of the Southern Scandinavian Ice Sheet.* Thesis, Oregon State University, Corvallis, OR.

Rinterknecht VR, Clark PU, Raisbeck GM, Yiou F, Bitinas A, Brook EJ, Marks L, Zelcs V, Lunkka J-P, Pavlovskaya IE, Piotrowski JA, Raukas A. 2006. The last deglaciation of southeastern sector of the Scandinavian Ice Sheet. *Science* **311**: 1449–1452.

Rinterknecht VR, Pavlovskaya IE, Clark PU, Raisbeck GM, Yiou F, Brook EJ. 2007. Timing of the last deglaciation in Belarus. *Boreas* **36**: 307–313.

Stone JO. 2000. Air pressure and cosmogenic isotope production. *Journal of Geophysical Research* **105**: 23753–23759.

Stone JO, Balco GA, Sugden DE, Caffee MW, Sass LC III, Cowdery SG, Siddoway C. 2003. Holocene deglaciation of Marie Byrd Land, West Antarctica. *Science* **299**: 99–102.

Ten Brink NW. 1972. Holocene chronology of Greenland Ice Sheet fluctuations in the Søndre Strømfjord region of West Greenland. In *Programs, Geological Society of America Abstract with Programs*, 4: 416.

Ten Brink NW. 1974. Glacio-isostasy: new data from West Greenland and geophysical implications. *Geological Society of America Bulletin* **85**: 219–228.

Ten Brink NW. 1975. Holocene history of the Greenland ice sheet based on radiocarbon-dated moraines in West Greenland. *Meddelelser om Grønland* **201**: 1–44.

Thomas ER, Wolff EW, Mulvaney R, Steffensen JP, Johnsen SJ, Arrowsmith C, White JWC, Vaughn B, Popp T. 2007. The 8.2 ka event from Greenland ice cores. *Quaternary Science Reviews* **26**: 70–81.

Van Tatenhove FGM, Van Der Meer JJM, Huybrechts P. 1995. Glacial-geological/geomorphological research in west Greenland used to test an ice-sheet model. *Quaternary Research* **44**: 317–327.

Van Tatenhove FGM, Van Der Meer JJM, Koster EA. 1996. Implications for deglaciation chronology from new AMS age determinations in central west Greenland. *Quaternary Research* **45**: 245–253.

Waelbroeck C, Labeyrie L, Michel E, Duplessy JC, McManus JF, Lambeck K, Balbon E, Labracherie M. 2002. Sea-level and deep water temperature changes derived from benthic foraminifera isotopic records. *Quaternary Science Reviews* **21**: 295–305.

Wahr J, Van Dam T, Larson K, Francis O. 2001. Geodetic measurements in Greenland and their implications. *Journal of Geophysical Research* **106**(16): 567–581.

Weidick A. 1968. Observations on some Holocene glacier fluctuations in West Greenland. *Meddelelsser om Grønland* **165**: 1–203.

Weidick A. 1972. *Holocene shore-lines and glacial stages in Greenland: an attempt at correlation.* Rapport 41, Grønlands Geologiske Undersøgelse, Copenhagen.

Weidick A. 1995. Greenland. In *Satellite Image Atlas of Glaciers of the World.* US Geological Survey Professional Paper 1386-C, Washington, DC; 1–153.

Weidick A, Oerter H, Reeh N, Thomsen HH, Thoring L. 1990. The recession of Inland Ice margin during the Holocene climatic optimum in the Jaconshavn Isfjord area of West Greenland. *Palaeogeography, Palaeoclimatology, Palaeoecology* **82**: 389–399.

Willemse NW. 2002. Holocene sedimentation history of the shallow Kangerlussuaq lakes, west Greenland. *Meddelelser om Grønland* **41**: 1–48.

Willemse NW, Koster EA, Hoogakker B, van Tatenhove FGM. 2003. A continuous record of Holocene eolian activity in West Greenland. *Quaternary International* **59**: 322–334.

Yokoyama Y, Lambeck K, De Deckker P, Johnston P, Fifield LK. 2000. Timing of the Last Glacial Maximum from observed sea-level minima. *Nature* **406**: 713–716.

DOI: 10.1002/jqs